Revue des Composites et des Matériaux Avancés-Journal of Composite and Advanced Materials
Vol. 35, No. 3, June, 2025, pp. 559-566
Journal homepage: http://iieta.org/journals/rcma

Enhancing Composite Freeze-Dried Chitosan/TPP Hydrogel Scaffolds with nGO and nHAp for Bone Tissue Engineering

Nadeen J. Ismael*, Ishraq Abd Ulrazzaq Kadhim, Basma H Al-Tamimi

Collage of Materials of Engineering, University of Technology-Iraq, Baghdad 10066, Iraq

Corresponding Author Email: 130206@uotechnology.edu.iq

https://doi.org/10.18280/rcma.350316

Received: 9 May 2025
Revised: 10 June 2025
Accepted: 22 June 2025
Available online: 30 June 2025

Keywords:
bone tissue engineering, chitosan, freeze-drying, nano graphene oxide, nanohydroxyapatite, tripolyphosphate

ABSTRACT

Bone tissue engineering seeks to create methods for repairing sick or injured bone by combining cells, growth factors, and biomaterials. This work studies the creation and improvement of freeze-dried chitosan-based hydrogel scaffolds crosslinked with tripolyphosphate TPP and enriched with graphene oxide nGO and nanohydroxyapatite nHAp for bone tissue engineering applications. Swelling ratio, FTIR, degradation, contact angle, SEM, and antibacterial test were among the physical, chemical, and biological examinations used to characterize the scaffolds, which were made in varying compositions. With higher chitosan and nGO/nHAp concentrations, the results showed enhanced degradation resistance, good swelling behavior, and the chemical bonding was improved. Good mechanical enhancement, biocompatibility, and antibacterial activity specially against Gram-positive bacteria are achieved by the inclusion of nGO and nHAp. The suggested scaffolds' structural stability, advantageous hydrophilicity, and effective bioactivity make them promising candidates for bone regeneration applications, according to these findings.

1. INTRODUCTION

All over the world, the incidence of diseases and disorders relating to the bones has sharply increased in recent years [1]. Bone grafts are often necessary for surgical intervention for bone abnormalities caused by tumors, trauma, or aberrant development [2]. Because bone is a detailed three-dimensional structure that gives each mechanical support and a biological surrounding environment. So, a scaffold should mimic the extra cellular matrix (ECM) and follow particular biological and mechanical necessities to assemble and guide cells that create bone [3]. In bone tissue engineering, a biodegradable scaffold is a temporary skeleton implanted into the areas of missing or faulty bone used as a physical support and induce bone tissue regeneration as it progressively degrades and gets replaced by fresh bone tissue [4, 5].

Due to the extensive use of scaffolds in tissue engineering, materials with broad applicability and strong biocompatibility that are appropriate for scaffold fabrication are constantly being sought after [6]. These materials are supposed to momentarily fill the function of the ECM in the developing tissue by supporting cellular adhesion and deposition of mineralized matrix and usually built as a scaffold [7, 8]. The scaffold's primary function is to replicate the natural environment's design, which includes skin, cartilage, bone, and muscles, and to ensure biological function that promotes cell attachment and the creation of new tissue [9]. Chitosan (CS) attracted a lot of interest because of its biocompatibility, bioactivity, low cost, and environmentally friendly characteristics; above all, though, their presence of functional groups useful to improve their biological and mechanical properties [10]. Chitosan is a polysaccharides polymer derived from natural sources, mostly it comes from the exoskeletons of marine animals like lobsters and crabs [11, 12]. Chitosan still shows low cell adherence and is mechanically weak. So, it reinforced with crosslinking agents to increase the mechanical characteristics and stability, therefore enhancing the strength and slowing down the rate of scaffold disintegration [13]. Since phosphate groups are considered important for bone mineralization and for evolution of biomimetic polymer systems for bone regeneration, Tripolyphosphate (TPP) is used as an anionic crosslinkers agent for chitosan [14]. TPP molecules are negatively charged that produce polyelectrolyte complexes generally harmless and biocompatible by combining three phosphate groups with the free amine groups of positively charged chitosan molecules [15]. The following figure shows the reaction occur between chitosan and tripolyphosphate [16].

Graphene oxide (GO) contains oxygen functional groups that are affixed to the edges of the plane and both sides of the layered carbon structure [17, 18]. Numerous hydrophilic functional groups found in GO, such as hydroxyl, carboxyl, and epoxy groups, help to improve the biocompatibility by enabling additional chemical modification with biomolecules like proteins and polysaccharides [19, 20]. Since nHAp is a crucial component for bone regeneration and is frequently employed as a filler to encourage bone growth, it is vital to replicate the physicochemical characteristics of nHAp in

human bone [21]. The biocompatibility, high osteoconductivity, osteoinductivity, and biological activity of nHAp make it one of the biomaterials that is expected to be used for bone tissue engineering [22].

Porous chitosan/TPP hydrogels scaffolds reinforced with nano graphene oxide nGO and nanohydroxyapatite nHAp were created using freeze-drying method. The approach of freeze-drying is particularly utilized for creating porous materials, since non-toxic water is typically used [23].

Valencia et al. [24] prepared scaffolds using chitosan and graphene oxide in three different formulas (nGO 0%, 0.5%, and 1%) by freeze-drying method. SEM, FTIR, and TGA tests were used to characterize the scaffolds. The findings indicate that stability improved as the amount of nGO increased. The scaffolds were biocompatible and tissue architecture recovery were demonstrated upon their implantation.

Although bone tissue engineering has made great strides in the manufacturing of scaffolds, there are still difficulties regarding balancing between making scaffolds with high mechanical qualities, excellent biocompatibility, and also being biodegradable. On this basis, this work studies the improvement of scaffolds made of chitosan built of TPP crosslinker and reinforced with nGO and nHAP, depending on the freeze-drying technique through series of physical and chemical examinations to adjust the structural and porous properties. Few studies have examined the synergistic benefits of using graphene oxide and hydroxyapatite together in a TPP-crosslinked freeze-dried system, despite the fact that both materials have been separately included into chitosan-based scaffolds in the past. By methodically examining how the addition of nGO and nHAp improves the physical and chemical characteristics of chitosan/TPP hydrogels for bone tissue engineering, this study attempts to close this gap.

2. MATERIALS AND METHODS

2.1 Materials

Chitosan (CS) was obtained from Xi'an Shaanxi (China) at 75% degree of deacetylation and a molecular weight of 161 g/mol; acetic acid (99%) was purchased from Chem-lab NV (Belgium); TPP was purchased from Sigma-Aldrich Co., Germany; phosphate buffer saline (PBS) with a pH of 7.2 was purchased from HIMEDIA (India); and lysozyme (LZ, ≥ 90% proteins, activity ≥ 40,000 U/mg) was also obtained from CDH (India); Nano-graphene oxide powder (thickness:3.4nm, diameter:10-50µm, layer:5-10) (Xi'an Shaanxi, China); HA (purity 97%, 20 nm particle size) was purchased from Aladdin (Shanghai, China).

2.2 Preparation of CS/TPP crosslinker+nGO/nHAp hydrogel

2.2.1 Preparation of (CS+TPP crosslinker) hydrogel

In a beaker, 25 ml of distilled water mixed with 5 ml of acetic acid and placed on the magnetic stirrer, and then different concentrations of chitosan (6%, 13%, 20%) w/v added gradually and stirred at 1400 rpm without heat for 2 hours until the solution become homogenous and all chitosan powder dissolved. The TPP crosslinker to chitosan weight ratio added to each of the prepared solution and stirred for 1hour was 1:40 (w/w). Initial research and literature publications that highlighted these ranges as indicative of low, moderate, and high chitosan contents employed in hydrogel scaffold production led to the choice of 6%, 13%, and 20% (w/v) chitosan concentrations [6, 11]. These concentrations make it possible to assess the effects of chitosan content on mechanical behavior, degradation, porosity, and viscosity. Higher concentrations increase the integrity of the structure but may decrease permeability, whereas lower amounts promote more porosity and swelling.

2.2.2 Addition of nGO and nHAp to hydrogel

After the preparation of the three different CS/TP hydrogel, they were enriched with graphene oxide and hydroxyapatite. The addition of nano graphene oxide and nano hydroxyapatite was (0.1g nGO and 0.3g HAp) and (0.1g HAp and 0.3g nGO). Hydrogel solutions were poured in cubical rubber molds, (1cm × 1cm), frozen at -20°C overnight and then lyophilized for 12 hours at -80°C and 0.05 mbar. It should be made clear that all three group (A, B, and C) in this investigation has a baseline control scaffold (A1, B1, and C1 respectively) made of only chitosan crosslinked with TPP, free of nGO or nHAp. These control samples are used as benchmarks to separate and contrast how adding nGO and/or nHAp affects the physical and chemical, characteristics. A thorough assessment of the additives individually and overall effects was made possible by the experimental design, which was set up to allow for simple comparisons within each concentration level. The chitosan-based scaffolds shown in the Figure 1.

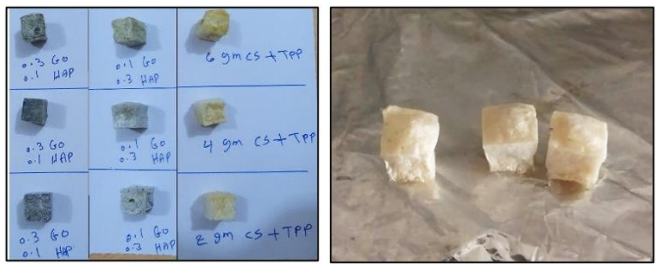

Figure 1. The prepared chitosan-based scaffolds

2.3 Analysis and evaluation methods

2.3.1 Scanning Electron Microscopy (SEM)

One essential examination used for studying the surface structure and micromorphology of the scaffolds was scanning electron microscopy test. The model of this device is (Inspect S 50). It is made by (FEI-Netherlands). This device is available at the University of Technology/ Nanotechnology and Advanced Materials Research Center.

2.3.2 Fourier Transform Infrared Spectroscopy (FTIR)

The FTIR spectra were obtained on FTIR microscopy (Bruker, Germany) to find the vibration of function groups of the scaffolds throughout the 4000–400 cm-1 range by employing the KBr disk technology.

2.3.3 Swelling ratio

Based on ASTM D4546-08, the swelling ratio of scaffolds was evaluated. The scaffolds were immersed in solution of (PBS) pH 7.2 for 24h at room temperature. The excess water was removed using tissue paper and the samples left to dry for couple of hours, then the weight was recorded. The swelling ratio was determined via the following Eq. (1) [12]:

$$Swelling\ ratio\ (\%) = \frac{W - W_o}{W_o} \times 100 \qquad (1)$$

where, W_o the wight of dried sample and W the wight of swollen one.

2.3.4 Contact angle

To improve cell adhesion to the scaffold, one must first be aware of the longest time needed for scaffold to become more hydrophilic. The technique involves ASTM standard D5946-04 measurement of contact angle of the water droplet on scaffold surface using Young-Laplace fitting method.

2.3.5 Degradation degree

By weighing the dry samples (W_o), the deterioration rate of scaffolds with dimensions 1 cm × 1 cm. The scaffolds were immersed in PBS solution with lysozyme 0.0001g/L and cultured at 37℃ for up to five weeks, with a fresh degradation medium every third day. Following every week of incubation, the scaffolds were taken out of the degradation media, cleaned with distilled water, then dried at room temperature. Weighing the dry scaffolds was noted as W_d, the degradation rate of the scaffolds was computed by the following Eq. (2) [12]:

$$Weight\ lose\ (\%) = \frac{W_o - W_d}{W_o} \times 100 \qquad (2)$$

where, W_o the wight of dried sample and W_d the dry weight after degradation.

2.3.6 Bacterial inhibition assessment

Two types of bacteria used Gram-positive Staphylococcus aureus and Gram-negative Pseudomonas aeruginosa to evaluate the ability of the scaffolds for reduction of bacteria growth and examine the inhibition regions. The examination procedure used according to the following researches [25, 26].

2.3.7 Data analysis

For each sample group, all experiments were carried out in triplicate (n = 3) to guarantee statistical reliability and reproducibility. The data are displayed by mean standard deviation ± (SD). The results were graphed using the OriginPro 2024 program. The significance of group differences was assessed using one-way analysis of variance (ANOVA), with a significance level of $p < 0.05$. The study groups in our investigation were organized using a rational and methodical approach comparable to a semi-factorial design. This produced nine different formulations of scaffold, which enabled us to assess the impact of chitosan percentage and nano-additive composition alone and in combination on scaffold performance. Further research might use CFU-based quantification to improve the analytical evaluation of bacterial decrease, even though zone of inhibition measures were employed for antibacterial assessment.

3. RESLTS AND DISCUSSION

Physiochemical tests were used in this work to assess the qualities of the manufactured scaffolds. A comprehensive investigation of these results is given in the sections that follow.

3.1 Scanning Electron Microscopy (SEM)

The morphological characteristics and structural shape of interconnected pores and pore sizes of the chitosan-based scaffold were examined by SEM at different points on the cross-sectional surface.

The images with higher magnification show an uneven distribution of big pores, with the pores appearing comparatively wider and larger. While the images with lower magnification shows more intricate details of the pores and makes it evident that there is a range of sizes, including smaller ones. Since smaller pores promote cell adherence and larger pores allow material flow, this variation in sizes of pores may have particular purposes, such as promoting cell growth at several levels. The overall structure supports the creation of a cohesive material by showing that chitosan/TPP have good interfacial contact with nGO/nHAp. The scaffolds have curved surface patterns and high porosity that make it seem appropriate for promoting cell growth. Since the freeze-drying process effectively created a three-dimensional porous network, the chitosan-based scaffolds are suitable for bone tissue engineering. Although this study did not conduct specific mechanical testing (compressive strength), SEM data and existing literature supported the inference that the scaffolds had improved mechanical behavior. SEM results showed that scaffolds incorporating nGO and nHAp have improved pore interconnectivity and structural integrity. Prior research has shown that adding nGO and nHAp to chitosan-based scaffolds greatly increases their mechanical strength via the formation of hydrogen bonds, improved crystallinity, and inorganic phase reinforcement [27-29]. The SEM images of the prepared chitosan-based scaffolds shown in Figure 2.

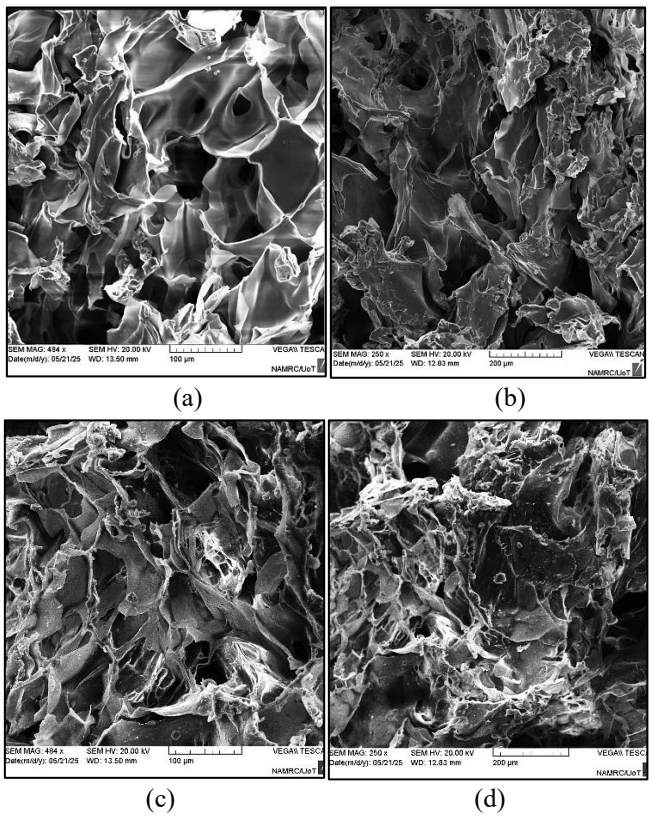

Figure 2. SEM images of the scaffold: (a, b) B1(13%CS/TPP): displays big, irregularly edged macropores that are linked, (c, d) for B2(13%CS/TPP + 0.1g nGO+0.3 nHAp): shows denser scaffold walls and more consistent pore structures, suggesting enhanced structural integrity brought about by nano-additive reinforcement

Although SEM offered useful information about the surface

morphology and pore structure of the scaffolds, this study did not quantitatively analyze the distribution of pore sizes or total porosity. The observed range of pore sizes, from larger interconnected macropores to smaller micropores, is in line with designs that are known to facilitate cell infiltration and nutrient diffusion [9]. Software for image processing will be used in future research to measure the distribution of pore sizes and porosity. Compressive strength will be used in future research to precisely confirm the noted structural improvements in mechanical durability.

3.2 Fourier transformation infrared spectroscopy (FTIR)

It was found that all groups had similar spectral patterns with only little variation in peaks intensity. Therefore, the results will be discussed and interpreted based on one group specially B1, B2, B3 group and the same interpretation for the other two groups.

Although pure chitosan was not subjected to FTIR analysis in this investigation, previously published spectra served as a guide for comparison. Pure chitosan usually exhibits distinctive peaks at 3290 cm^{-1} (O–H/N–H stretching), 1595 cm^{-1} (amide I), and 1150 cm^{-1} (C–O–C stretching), according to this research [30]. The B1 group (CS13%/TPP) in the current study showed additional peaks at ~1214 cm^{-1} and ~1148 cm^{-1}, which are linked to phosphate bonds, and at ~1093 cm^{-1}, which corresponds to –P–O vibrations. The creation of crosslinking through ionic interactions is confirmed by these peaks, which show that tripolyphosphate (TPP) was successfully incorporated into the chitosan structure.

B2 (CS13%/TPP + 0.1g nGO + 0.3g nHAp) exhibits additional peaks because nGO and nHAp are included. The weakest new peaks appear at approximately 870 cm^{-1} [31], indicating the association of hydroxyapatite (PO_4^{3-}). The vibrations associated with -P-O and HAp intensify the peaks at about 1040–1100 cm^{-1} [27]. Increased nGO–CS connections may be the cause of the small increase in absorption at ~1620–1650 cm^{-1}. The concentration of nGO is indicated by the more noticeable peaks in B3 (CS13%/TPP + 0.3g nGO + 0.1g nHAp) about 1040–1100 cm^{-1}. Because nGO encourages hydrogen bonding, its presence may result in an increase in the absorption spectrum between around 2900 and 3500 cm^{-1} [28]. The FTIR pattern of the prepared chitosan-based scaffolds shown in Figure 3.

3.3 Swelling ratio test

The swelling behavior is essential for the effectiveness of bone healing because in hydrogels, pores may collapse as a result of the polymer swelling [32]. SEM images (Figure 2) support this, showing that the denser structure brought about by nGO and nHAp restricts excessive swelling, while interconnecting holes encourage water absorption. The immersed scaffolds shown in Figure 4, and the scaffolds formulations are the same as those described in Figure 5. Figure 4 displays chitosan-based scaffolds immersed in PBS solution, pH 7.2 for 24 hours at room temperature to evaluate the swelling ratio.

Figure 5 shows the swelling ratio results of the prepared chitosan-based scaffolds. The data is presented as mean ± SD, with n = 3. A1(CS6%/TPP), A2(CS6%/TPP + 0.1g nGO+0.3g nHAp), A3(CS6%/TPP + 0.3g nGO+0.1g nHAp). Since chitosan has a high water-binding affinity and abs orption capacity because of its hydroxyl and amine groups, we see that chitosan concentration controls the swelling ratio, as it is higher in groups B and C than that of group A. Because of the structural and porosity changes brought about by the addition of nGO and nHAp, a slight decrease in swelling accrued.

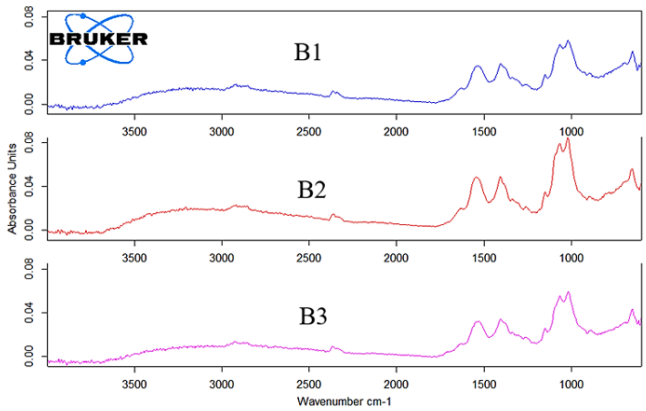

Figure 3. FTIR for B1(CS13%/TPP), B2(CS13%/TPP + 0.1g nGO+0.3g nHAp) and B3(CS13%/TPP + 0.3g nGO+0.1g nHAp) scaffolds. Among those with labels are ~3290 cm^{-1} (O–H/N–H stretch), ~1595 cm^{-1} (Amide I), ~1040–1100 cm^{-1} (PO_4^{3-} / P–O), ~870 cm^{-1} (HAp), and ~1214, 1148 cm^{-1} (TPP phosphate bonding)

Figure 4. Chitosan-based scaffolds immersed in PBS solution, pH 7.2 for 24h at room temperature to evaluate the swelling ratio

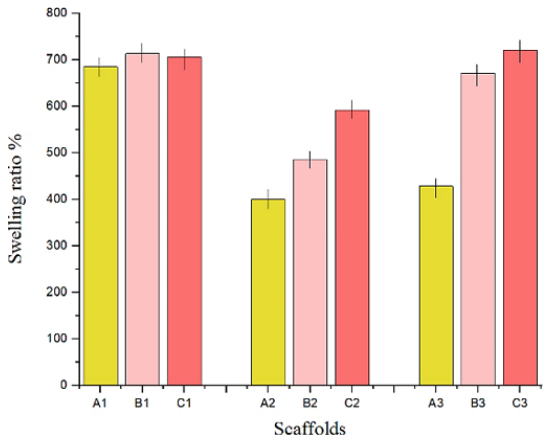

Figure 5. The swelling ratio results of the prepared chitosan-based scaffolds (Note: The data is presented as mean ± SD, with n = 3. A1(CS6%/TPP), A2(CS6%/TPP + 0.1g nGO+0.3g nHAp), A3(CS6%/TPP + 0.3g nGO+0.1g nHAp), B1(CS13%/TPP), B2(CS13%/TPP + 0.1g nGO+0.3g nHAp), B3(CS13%/TPP + 0.3g nGO+0.1g nHAp), C1(CS20%/TPP), C2(CS20%/TPP + 0.1g nGO+0.3g nHAp), C3(CS20%/TPP + 0.3g nGO+0.1g nHAp))

Due to the impact of these additives on the porous network structure, the incorporation of 0.1g nGO and 0.3g nHAp

resulted in a slight reduction in swelling ratio. However, adding 0.3g nGO and 0.1g nHAp has a similar effect but led to a slightly higher swelling ratio. This suggests a balancing effect between porosity and chemical composition adjustments, which may help improve the material's mechanical stability and reduce undesirable excessive swelling.

3.4 Contact angle test

Because cell adhesion is typically increased on hydrophilic surfaces and to disclose the osteoblast response to the total biomaterial wettability, the wettability of biomaterials is of fundamental concern in tissue engineering [33].

The addition of nGO and nHAp resulted in a minor variation, making Group A samples with contact angles (51.4°, 58.2°, 59.3°) the least effective in terms of hydrophilicity. In contrast, the change in contact angles within Group A samples was consistent and gradual [34]. While the higher chitosan content, Group B samples with contact angles (54.4°, 75°, 60.5°) displayed distinct outcomes and a wider range of contact angles. The hydrophilicity within this group varied significantly due to the ratios used and the effect of adding nGO and nHAp [35]. Group C samples with contact angles (67.8°, 53.4°, 57.6°) was the most effective for promoting bone cell adhesion, stimulate cell development and proliferation, and improve biological fluid absorption due to its favorable hydrophilic behavior [36]. It is suitable for bone tissue fabrication as it combines high fluid absorption with a balance structural stability. Figure 6 shows the contact angles data results of the scaffolds.

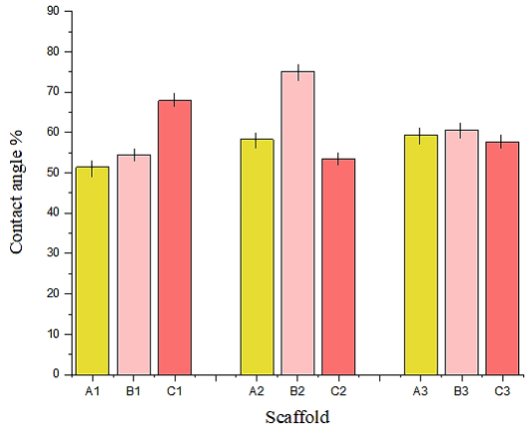

Figure 6. Contact angles result of the prepared chitosan-based scaffolds (Note: The data is presented as mean ± SD, with n = 3. A1(CS6%/TPP), A2(CS6%/TPP + 0.1g nGO+0.3g nHAp), A3(CS6%/TPP + 0.3g nGO+0.1g nHAp), B1(CS13%/TPP), B2(CS13%/TPP + 0.1g nGO+0.3g nHAp), B3(CS13%/TPP + 0.3g nGO+0.1g nHAp), C1(CS20%/TPP), C2(CS20%/TPP + 0.1g nGO+0.3g nHAp), C3(CS20%/TPP + 0.3g nGO+0.1g nHAp))

3.5 Degradation degree test

One of the most crucial tests in bone tissue engineering is the degree of degradation, since the scaffold must gradually degrade to allow time for new tissue to grow [37]. The four-week duration of the degradation study is consistent with a number of earlier investigations that examined the early biodegradation behavior of scaffolds based on chitosan [12, 36]. In order to estimate the scaffold's first few months after implantation, this period of time was chosen to evaluate initial stages stability and material loss. Since chitosan is known to break down a little quickly in enzymatic settings, the four-week interval made it possible to clearly observe how different formulations differed from one another. Future research will examine extended degradation kinetics in simulated in vivo settings over longer time periods. Table 1 shows the wight of the scaffolds through four weeks and wight lose%.

Table 1. The resulted data from degradation test of chitosan-based scaffolds

Samples	Week 1 (g)	Week 2 (g)	Week 3 (g)	Week 4 (g)	Wight Lose%
A1	0.057	0.0472	0.0374	0.0283	59.57
A2	0.0605	0.0542	0.0472	0.0402	49.75
A3	0.0591	0.0514	0.0438	0.0353	49.57
B1	0.0584	0.0497	0.0402	0.0332	58.50
B2	0.0619	0.0569	0.0511	0.0444	36.57
B3	0.0605	0.0538	0.0465	0.0395	43.57
C1	0.0598	0.0528	0.0444	0.0374	76.63
C2	0.0633	0.0589	0.0546	0.0479	60.08
C3	0.0619	0.0563	0.0499	0.0451	65.31

The scaffolds with only chitosan/TPP showed higher rates of weight loss and biodegradation than those with the additives (nGO+nHAp). It also found that scaffolds with higher chitosan concentration have more resistance to enzyme diffusion because of the increased structural density, thus led to lower wight lose and degradation. Figure 7 shows the immersed scaffolds in PBS solution with lysozyme. The degradation resistance improved further with adding (nGO+nHAp) as they greatly enhanced the stability of the scaffolds. nHAp physically fills the pore structure of the scaffolds and nGO create hydrogen bond with chitosan which both lead to lower degradation degree [29, 38]. Figure 8 shows the resulted degradation data of the scaffolds. Our formulations, particularly those containing nGO and nHAp, exhibit better degradation resistance in comparison to comparable chitosan-based scaffolds documented in previous research [12, 36], indicating increased structural stability.

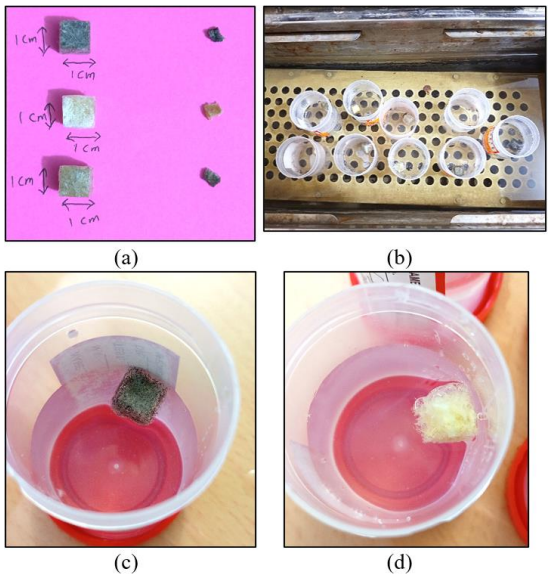

Figure 7. (a) The scaffolds dimensions before and after losing weight, (b), (c), and (d) Chitosan-based scaffolds immersed in PBS solution with lysozyme 0.0001g/L and cultured at 37°C to evaluate the degradation

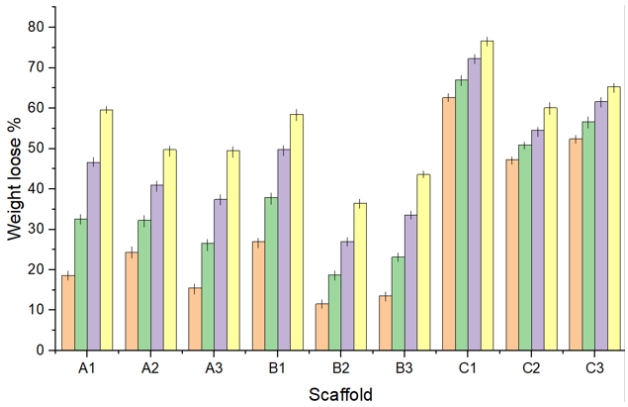

Figure 8. Degradation results of the prepared chitosan-based scaffolds through four weeks (Note: The data is presented as mean ± SD, with n = 3. A1(CS6%/TPP), A2(CS6%/TPP + 0.1g nGO+0.3g nHAp), A3(CS6%/TPP + 0.3g nGO+0.1g nHAp), B1(CS13%/TPP), B2(CS13%/TPP + 0.1g nGO+0.3g nHAp), B3(CS13%/TPP + 0.3g nGO+0.1g nHAp), C1(CS20%/TPP), C2(CS20%/TPP + 0.1g nGO+0.3g nHAp), C3(CS20%/TPP + 0.3g nGO+0.1g nHAp))

Following a month of biodegradation testing, a one-way ANOVA was used to determine whether the weight loss percentages for all the scaffolds differed statistically significantly. Each group's weight loss values were as follows:

for Group A (49.57% to 59.57%)

for Group B between (36.57% and 58.50%)

for Group C (76.63% to 60.08%)

The ANOVA test showed a significant distinction between the groups ($p < 0.05$), suggesting that the degradation rate was significantly influenced by the scaffold composition. The groups' differences in weight loss are shown in Figure 9, with Group C showing the highest rate of degradation, followed by Groups A and B.

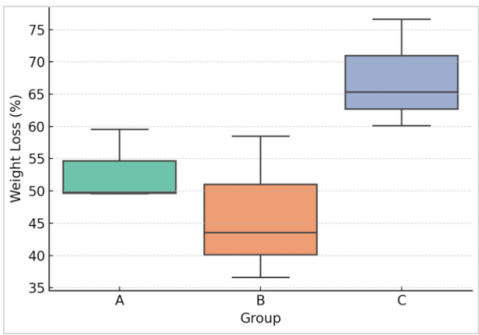

Figure 9. Weight loss (%) of chitosan-based Scaffold following four weeks of biodegradation

The spread and apparent inhibition zones surrounding the holes in each dish in the image can be used to evaluate the impact of both types of bacteria, Gram-positive (Staphylococcus aureus) and Gram-negative (Pseudomonas aeruginosa). Certain areas of the samples in the upper dishes showed distinct inhibitory zones for Gram-positive bacteria (S. aureus). The majority of them were successful in lowering bacterial growth, despite the fact that not all scaffolds had the same resistance to the growth of Gram-positive bacteria [39]. Adding nHAp and nGO to chitosan scaffolds improves their antibacterial property [40]. Figure 10 shows the antibacterial test dish. The complimentary mechanisms of nGO and nHAp in scaffolds are responsible for their antibacterial action. While nHAp releases ions called Ca^{2+} and PO_4^{3-} that destabilize bacterial cell walls, nGO can damage bacterial membranes through oxidative stress and sharp edges [20, 38, 39]. Because of their simpler wall construction, Gram-positive bacteria are more susceptible to these effects, which explains why their inhibition zones are greater than those of Gram-negative species.

Since Gram-positive microorganisms can cause infections in tissue engineering applications, this is seen as a good indicator. Comparing the lower plates to the higher dishes, the effect against Gram-negative bacteria (P. aeruginosa) revealed smaller inhibitory zones and a less noticeable reaction. Given that the cell walls of Gram-negative bacteria are thicker and more complexly structured than those of Gram-positive bacteria, this pattern suggests that the bacteria are more resistant to the antimicrobial agents found in the samples. Gram-positive bacteria have a thick peptidoglycan layer that is easier to target, but Gram-negative bacteria have an outer barrier that makes it harder for antibiotics to enter. This difference in cell wall composition explains these results. Table 2 shows the bacterial inhibition zone.

Despite the absence of in vitro or in vivo biocompatibility testing, such as proliferation or cell viability experiments, in this study, the physiochemical characterizations show favorable circumstances for cell adhesion and growth. The enhanced hydrophilicity, antimicrobial activity, and porosity of the scaffolds improve their biological efficacy. Future research will concentrate on carrying out thorough biological assessments, such as live/dead cell staining and MTT assays, to validate these scaffolds' biocompatibility and regeneration potential.

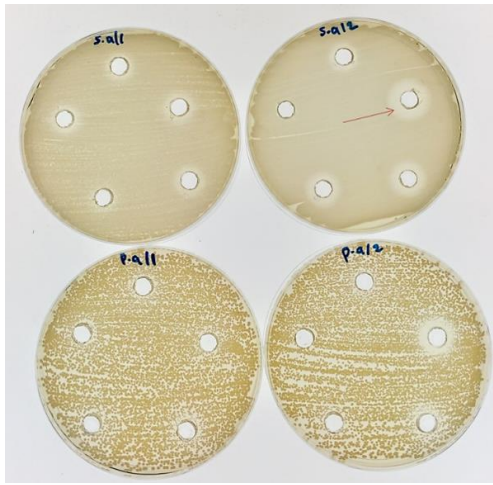

Figure 10. Antibacterial test for Gram-positive (Staphylococcus aureus) for upper dish and Gram-negative (Pseudomonas aeruginosa) for the lower dish

Table 2. Bacterial inhibition zone

Scaffolds	Inhibition Zone(mm)	
	Staphylococcus aureus	Pseudomonas
A1	12.2	9.3
A2	13	10.8
A3	13.6	10.5
B1	15.5	8.3
B2	14.3	9.7
B3	12.2	9.2
C1	18	14.5
C2	16.8	13.2
C3	17	12.7

4. CONCLUSSION

Using the freeze-drying method, this work effectively produced hydrogel scaffolds based on chitosan that were reinforced with nGO and nHAp. To encourage bone tissue regeneration, biochemical, mechanical, and structural properties must be adjusted. The results revealed that the scaffolds' capacity to expand, sustain degradation, and resist bacteria was much enhanced by the addition of nGO/nHAp and an increase in chitosan content. In order to improve bone cell proliferation and reduce the danger of infection, the scaffolds display a desirable balance between durability and hydrophilicity when the concentration of nGO is increased. These findings present beneficial knowledge for the development of bioactive scaffolds and establish the potential benefits of composite chitosan/TPP/nGO/nHAp hydrogels. To further optimize and quantitatively model formulation parameters, we plan to use complete factorial or response surface methodology (RSM) designs with specialized DOE software in subsequent work. The scaffolds regeneration ability will be validated by future biological validation, which will include osteogenic differentiation experiments and the MTT assay.

REFERENCES

[1] Swetha, M., Sahithi, K., Moorthi, A., Srinivasan, N., Ramasamy, K., Selvamurugan, N. (2010). Biocomposites containing natural polymers and hydroxyapatite for bone tissue engineering. International Journal of Biological Macromolecules, 47(1): 1-4. https://doi.org/10.1016/j.ijbiomac.2010.03.015

[2] Shi, H., Zhou, Z.Q., Li, W.D., Fan, Y., Li, Z.H., Wei, J.C. (2021). Hydroxyapatite based materials for bone tissue engineering: A brief and comprehensive introduction. Crystals, 11(2): 149. https://doi.org/10.3390/cryst11020149

[3] Ma, P.F., Wu, W.J., Wei, Y., Ren, L., Lin, S.X., Wu, J.H. (2021). Biomimetic gelatin/chitosan/polyvinyl alcohol/nano-hydroxyapatite scaffolds for bone tissue engineering. Materials & Design, 207: 109865. https://doi.org/10.1016/j.matdes.2021.109865

[4] Li, Z., Ramay, H.R., Hauch, K.D., Xiao, D., Zhang, M. (2005). Chitosan—Alginate hybrid scaffolds for bone tissue engineering. Biomaterials, 26(18): 3919-3928. https://doi.org/10.1016/j.biomaterials.2004.09.062

[5] Zhang, Y., Ni, M., Zhang, M.Q., Ratner, B. (2003). Calcium phosphate—Chitosan composite scaffolds for bone tissue engineering. Tissue Engineering, 9(2): 337-345. https://doi.org/10.1089/107632703764664800

[6] Yang, B., Li, X.Y., Shi, S., Kong, X.Y., Guo, G., Huang, M.J., Luo, F., Wei, Y.Q., Zhao, X., Qian, Z.Y. (2010). Preparation and characterization of a novel chitosan scaffold. Carbohydrate Polymers, 80(3): 860-865. https://doi.org/10.1016/j.carbpol.2009.12.044

[7] Koons, G.L., Diba, M., Mikos, A.G. (2020). Materials design for bone-tissue engineering. Nature Reviews Materials, 5(8): 584-603. https://doi.org/10.1038/s41578-020-0204-2

[8] Kadhim, I.A.U., Taeh, A.S., Abed, M.S. (2024). Sodium alginate substrate coated with PVA/Nanosilver composite nanofibers for skin tissue engineering. Revue des Composites et des Matériaux Avancés-Journal of Composite and Advanced Materials, 34(3): 305-313. https://doi.org/10.18280/rcma.340305

[9] Cheng, A., Schwartz, Z., Kahn, A., Li, X.Y., Shao, Z., Sun, M.Y., Ao, Y.F., Boyan, B.D., Chen, H.F. (2019). Advances in porous scaffold design for bone and cartilage tissue engineering and regeneration. Tissue Engineering Part B: Reviews, 25(1): 14-29. https://doi.org/10.1089/ten.teb.2018.0119

[10] Afra, S., Samadi, A., Asadi, P., Bordbar, M., Iloukhani, M., Rai, A., Aghajanpour, M. (2024). Chitosan crosslinkers and their functionality in 3D bioprinting to produce chitosan-based bioinks. Inorganic Chemistry Communications, 168: 112842. https://doi.org/10.1016/j.inoche.2024.112842

[11] Gholap, A.D., Rojekar, S., Kapare, H.S., Vishwakarma, N., Raikwar, S., Garkal, A., Mehta, T.A., Jadhav, H., Prajapati, M.K., Annapure, U. (2024). Chitosan scaffolds: Expanding horizons in biomedical applications. Carbohydrate Polymers, 323: 121394. https://doi.org/10.1016/j.carbpol.2023.121394

[12] Kadhim, I.A.U. (2023). Investigation of physochimechal and biological properties of composite sodium alginate for tissue engineering. Journal of Biomimetics, Biomaterials and Biomedical Engineering, 59: 11-20. https://doi.org/10.4028/p-a7ygw7

[13] Amini, A.R., Laurencin, C.T., Nukavarapu, S.P. (2012). Bone tissue engineering: Recent advances and challenges. Critical Reviews™ in Biomedical Engineering, 40(5): 363-408. https://doi.org/10.1615/CritRevBiomedEng.v40.i5.10

[14] Chen, X.Q., Wu, T., Bu, Y.N., Yan, H.Q., Lin, Q. (2024). Fabrication and biomedical application of alginate composite hydrogels in bone tissue engineering: A review. International Journal of Molecular Sciences, 25(14): 7810. https://doi.org/10.3390/ijms25147810

[15] Goh, C.Y., Lim, S.S., Tshai, K.Y., El Azab, A.W.Z.Z., Loh, H.S. (2019). Fabrication and in vitro biocompatibility of sodium tripolyphosphate-crosslinked chitosan—Hydroxyapatite scaffolds for bone regeneration. Journal of Materials Science, 54(4): 3403-3420. https://doi.org/10.1007/s10853-018-3087-5

[16] Silvestro, I., Francolini, I., Di Lisio, V., Martinelli, A., Pietrelli, L., Scotto d'Abusco, A., Scoppio,, A., Piozzi, A. (2020). Preparation and characterization of TPP-chitosan crosslinked scaffolds for tissue engineering. Materials, 13(16): 3577. https://doi.org/10.3390/ma13163577

[17] Biru, E.I., Necolau, M.I., Zainea, A., Iovu, H. (2022). Graphene oxide—Protein-based scaffolds for tissue engineering: Recent advances and applications. Polymers, 14(5): 1032. https://doi.org/10.3390/polym14051032

[18] Motiee, E.S., Karbasi, S., Bidram, E., Sheikholeslam, M. (2023). Investigation of physical, mechanical and biological properties of polyhydroxybutyrate-chitosan/graphene oxide nanocomposite scaffolds for bone tissue engineering applications. International Journal of Biological Macromolecules, 247: 125593. https://doi.org/10.1016/j.ijbiomac.2023.125593

[19] Mohammadrezaei, D., Golzar, H., Rezai Rad, M., Omidi, M., Rashedi, H., Yazdian, F., Khojasteh, A., Tayebi, L. (2018). In vitro effect of graphene structures as an osteoinductive factor in bone tissue engineering: A systematic review. Journal of Biomedical Materials Research Part A, 106(8): 2284-2343.

https://doi.org/10.1002/jbm.a.36422
[20] Farani, M.R., Zare, I., Mirshafiei, M., Gholami, A., Zhang, M., Pishbin, E., Ahn, J.E., Mohammadi, A., Imani, M., Lak, M., Shen, J.L., Kang, H., Huh, Y.S. (2025). Graphene oxide-engineered chitosan nanoparticles: Synthesis, properties, and antibacterial activity for tissue engineering and regenerative medicine. Chemical Engineering Journal, 509: 160852. https://doi.org/10.1016/j.cej.2025.160852
[21] Mo, X.J., Zhang, D.J., Liu, K.D., Zhao, X.X., Li, X.M., Wang, W. (2023). Nano-hydroxyapatite composite scaffolds loaded with bioactive factors and drugs for bone tissue engineering. International Journal of Molecular Sciences, 24(2): 1291. https://doi.org/10.3390/ijms24021291
[22] Rajula, M.P.B., Narayanan, V., Venkatasubbu, G.D., Mani, R.C., Sujana, A. (2021). Nano-hydroxyapatite: A driving force for bone tissue engineering. Journal of Pharmacy and Bioallied Sciences, 13(Suppl 1): S11-S14. https://doi.org/10.4103/jpbs.JPBS_683_20
[23] Wu, X., Liu, Y., Li, X., Wen, P., Zhang, Y., Long, Y., Wang, X., Guo, Y., Xing, F., Gao, J. (2010). Preparation of aligned porous gelatin scaffolds by unidirectional freeze-drying method. Acta Biomaterialia, 6(3): 1167-1177. https://doi.org/10.1016/j.actbio.2009.08.041
[24] Valencia, C., Valencia, C.H., Zuluaga, F., Valencia, M.E., Mina, J.H., Grande-Tovar, C.D. (2018). Synthesis and application of scaffolds of chitosan-graphene oxide by the freeze-drying method for tissue regeneration. Molecules, 23(10): 2651. https://doi.org/10.3390/molecules23102651
[25] Balouiri, M., Sadiki, M., Ibnsouda, S.K. (2016). Methods for in vitro evaluating antimicrobial activity: A review. Journal of Pharmaceutical Analysis, 6(2): 71-79. https://doi.org/10.1016/j.jpha.2015.11.005
[26] Gonelimali, F.D., Lin, J., Miao, W., Xuan, J., Charles, F., Chen, M., Hatab, S.R. (2018). Antimicrobial properties and mechanism of action of some plant extracts against food pathogens and spoilage microorganisms. Frontiers in Microbiology, 9: 1639. https://doi.org/10.3389/fmicb.2018.01639
[27] Mohandes, F., Salavati-Niasari, M.J.R.A. (2014). Freeze-drying synthesis, characterization and in vitro bioactivity of chitosan/graphene oxide/hydroxyapatite nanocomposite. RSC Advances, 4(49): 25993-26001. https://doi.org/10.1039/C4RA03534H
[28] Kosowska, K., Domalik-Pyzik, P., Krok-Borkowicz, M., Chłopek, J. (2019). Synthesis and characterization of chitosan/reduced graphene oxide hybrid composites. Materials, 12(13): 2077. https://doi.org/10.3390/ma12132077
[29] Zhang, J., Nie, J., Zhang, Q., Li, Y., Wang, Z., Hu, Q. (2014). Preparation and characterization of bionic bone structure chitosan/hydroxyapatite scaffold for bone tissue engineering. Journal of Biomaterials Science, Polymer Edition, 25(1): 61-74. https://doi.org/10.1080/09205063.2013.836950
[30] Younes, I., Rinaudo, M. (2015). Chitin and chitosan preparation from marine sources. Structure, properties and applications. Marine Drugs, 13(3): 1133-1174. https://doi.org/10.3390/md13031133
[31] Shaltout, A.A., Allam, M.A., Moharram, M.A. (2011). FTIR spectroscopic, thermal and XRD characterization of hydroxyapatite from new natural sources. Spectrochimica Acta Part A: Molecular and Biomolecular Spectroscopy, 83(1): 56-60. https://doi.org/10.1016/j.saa.2011.07.036
[32] Gibbs, D.M., Black, C.R., Dawson, J.I., Oreffo, R.O. (2016). A review of hydrogel use in fracture healing and bone regeneration. Journal of Tissue Engineering and Regenerative Medicine, 10(3): 187-198. https://doi.org/10.1002/term.1968
[33] Lim, J.Y., Donahue, H.J. (2004). Biomaterial characteristics important to skeletal tissue engineering. Journal of Musculoskeletal and Neuronal Interactions, 4(4): 396.
[34] Souza, A.P., Neves, J.G., da Rocha, D.N., Lopes, C.C., Moraes, Â.M., Correr-Sobrinho, L., Correr, A.B. (2022). Chitosan/Xanthan membrane containing hydroxyapatite/Graphene oxide nanocomposite for guided bone regeneration. Journal of the Mechanical Behavior of Biomedical Materials, 136: 105464. https://doi.org/10.1016/j.jmbbm.2022.105464
[35] Suo, L., Jiang, N., Wang, Y., Wang, P.Y., Chen, J.Y., Pei, X.B., Wang, J., Wan, Q.B. (2019). The enhancement of osseointegration using a graphene oxide/chitosan/hydroxyapatite composite coating on titanium fabricated by electrophoretic deposition. Journal of Biomedical Materials Research Part B: Applied Biomaterials, 107(3): 635-645. https://doi.org/10.1002/jbm.b.34156
[36] Liu, S.D., Li, Z.R., Wang, Q.X., Han, J., Wang, W.Y., Li, S.H., Liu, H.F., Guo, S.T., Zhang, J.C., Ge, K., Zhou, G.Q. (2021). Graphene oxide/chitosan/hydroxyapatite composite membranes enhance osteoblast adhesion and guided bone regeneration. ACS Applied Bio Materials, 4(11): 8049-8059. https://doi.org/10.1021/acsabm.1c00967
[37] Tajvar, S., Hadjizadeh, A., Samandari, S.S. (2023). Scaffold degradation in bone tissue engineering: An overview. International Biodeterioration & Biodegradation, 180: 105599. https://doi.org/10.1016/j.ibiod.2023.105599
[38] Dinescu, S., Ionita, M., Pandele, A.M., Galateanu, B., Iovu, H., Ardelean, A., Costache, M., Hermenean, A. (2014). In vitro cytocompatibility evaluation of chitosan/graphene oxide 3D scaffold composites designed for bone tissue engineering. Bio-medical Materials and Engineering, 24(6): 2249-2256. https://doi.org/10.3233/BME-141037
[39] Prakash, J., Prema, D., Venkataprasanna, K.S., Balagangadharan, K., Selvamurugan, N., Venkatasubbu, G.D. (2020). Nanocomposite chitosan film containing graphene oxide/hydroxyapatite/gold for bone tissue engineering. International Journal of Biological Macromolecules, 154: 62-71. https://doi.org/10.1016/j.ijbiomac.2020.03.095
[40] Khosalim, I.P., Zhang, Y.Y., Yiu, C.K.Y., Wong, H.M. (2022). Synthesis of a graphene oxide/agarose/hydroxyapatite biomaterial with the evaluation of antibacterial activity and initial cell attachment. Scientific Reports, 12(1): 1971. https://doi.org/10.1038/s41598-022-06020-1